1995ApJ...445L..23E

THE ASTROPHYSICAL JOURNAL, 445:L23–L26, 1995 May 20
© 1995. The American Astronomical Society. All rights reserved. Printed in U.S.A.

HIGH ANGULAR RESOLUTION SPECTROSCOPIC AND POLARIMETRIC IMAGING OF THE GALACTIC CENTER IN THE NEAR-INFRARED

A. ECKART, R. GENZEL, R. HOFMANN, B. J. SAMS, AND L. E. TACCONI-GARMAN
Max-Planck-Institut für extraterrestrische Physik (MPE), Giessenbachstrasse, D 85740 Garching bei München, Germany
Received 1995 January 17; accepted 1995 March 3

ABSTRACT

We present improved 0″.15 resolution K-band (2.2 μm) maps of the central 0.5 pc of the Galaxy as well as, for the first time, 0″.2 J-band (1.25 μm) images, 0″.2 K-band polarimetry, and 0″.4 images in the 2.058 μm He I emission and 2.29 μm CO band head absorption features. The new K-band maps reach K magnitudes of about 16 and resolve the previously found object at the position of the radio source Sgr A*(R) into a small cluster of compact sources. With one exception, their polarizations are similar to other sources in its vicinity and thus are probably caused by anisotropic foreground dust extinction in the Galactic plane. The Sgr A*(IR) complex does not exhibit any significant flux density variations at 2.2 μm on timescales of minutes or years. We therefore interpret Sgr A*(IR) as a small local clustering of luminous stars ($M_K \approx -3$) near/at the position of the compact radio source. The central IRS 16 complex and the bright source IRS 13 are dominated by bright, luminous He I stars and confirm the cluster of about a dozen He I stars found by Krabbe et al. (1991). There are also a dozen sources with $K \leq 12.5$ exhibiting CO band head absorption within a radius of 10″ of Sgr A*(IR). The drop in CO band head strength found by Sellgren et al. (1990) thus is most likely not caused by the disappearance of CO sources but by the additional presence of the bright early-type stars.

Subject headings: galaxies: nuclei – Galaxy: center — infrared: stars

1. INTRODUCTION

High-resolution near-infrared imaging with the MPE camera SHARP (0″.05 pixels, 12″.8 field of view; Hofmann et al. 1993) resolved the 2.2 μm emission in the central parsec (at 8.5 kpc, 1″ = 0.041 pc) into about 340 stars and gave the first evidence for an infrared counterpart [Sgr A*(IR)] of the compact radio source Sgr A*(R) (Eckart et al. 1992, 1993) which is the most likely candidate for a possible massive black hole at the center of our Galaxy (e.g., Lo 1989). Imaging spectroscopy revealed a small cluster of luminous and probably massive, blue supergiants (Allen, Hyland, & Hillier 1990; Krabbe et al. 1991). Sellgren et al. (1990) found evidence that the depth of the 2.3 μm CO band head absorption decreases in the central 10″, perhaps indicating a lack of late-type stars there. Understanding better the properties of Sgr A*(IR) and its relation to Sgr A*(R), as well as determining the identification and distribution of different types of stars in the central parsec, are of great importance for the analysis of the structure and evolution of the Galactic center stellar cluster (e.g., Bailey 1980; Allen 1987; Sellgren et al. 1990; Eckart et al. 1992, 1993, 1994; Herbst, Beckwith, & Shure, 1993; Close, McCarthy, & Melia 1995; Genzel, Hollenbach, & Townes 1994). For this purpose we have carried out new near-infrared broadband imaging, as well as, for the first time, narrow-band imaging of near-infrared spectral lines of the central 0.5 pc as well as K-band imaging polarimetry.

2. OBSERVATIONS AND DATA REDUCTION

The new observations were carried out with the MPE infrared high-resolution camera, SHARP (Hofmann et al. 1993) at the 3.5 m New Technology Telescope (NTT) of the European Southern Observatory (ESO) in La Silla, Chile, on 1993 August 3–6 and 1994 April 21–29. For the K- and J-band observations on 1994 April 27 the seeing conditions were exceptional: with a long exposure seeing of about 0″.3 (FWHM) and short exposure seeing and image motions of less than 0″.2 (integration times of ≤ 1.0 s), the NTT was operating almost diffraction limited at 2 μm. We used integration times of 1 s in the K-band and 1 and 2 s in the J-band. A contour map of the very central 3″.2 × 3″.2 field of the new K-band image is displayed in Figure 1 (see also Fig. 2 [Pl. L4]). For most of the spectroscopic and polarimetric observations, the long-exposure seeing was between 0″.8 and 1″.0 FWHM, and short-exposure seeing varied between 0″.3 and 0″.5 FWHM. A detailed description of our speckle image processing procedure is given in Eckart et al. (1993, 1994; see also Christou 1991).

2.1. *Narrow-Band Images*

In order to obtain images in the 2.058 μm He I $n = 2$ $^1P \rightarrow {}^1S$ and the 2.29 μm $v = 0 \rightarrow 2$ band head absorption, we used in 1993 August the SHARP circular variable filter (CVF, $\lambda/\delta\lambda = 60$). In 1994 April we used narrow-band filters (NBFs; $\lambda/\delta\lambda = 150$). For the CVF we chose central wavelengths of A: 2.093, B: 2.052, and C: 2.013 μm for the He I and V: 2.368, W: 2.326, X: 2.287, Y: 2.242, and Z: 2.198 μm for the CO band-head absorption. For the NBFs the central wavelengths are A: 2.042, B: 2.059, and C: 2.085 μm for the H I and A: 2.272, B: 2.295, and C: 2.318 μm for the CO band head absorption. The simple-shift-and-add (SSA) point-spread function (on IRS 7) consists of a sharp peak with a width of about 0″.2 centered on top of the SSA seeing background with a FWHM close to that of the short-exposure seeing. The deconvolved images (Lucy 1974) were then reconvolved with a Gaussian of FWHM 0″.4 as a clean beam. Maps of line emission and absorption were computed by subtracting the mean of the off-line channels from the on-line channel. In case of the CVF He I and all NBF data, the line maps were computed via $B - (A + C)/2$ where A, B, and C are the fluxes at the corresponding wavelengths. Due to the lower CVF resolution and the structure of the CO absorption features we processed the CVF CO data following $-(V + W + X) + (Y + Y + Z)$. The line-to-contin-

© American Astronomical Society • Provided by the NASA Astrophysics Data System

1995ApJ...445L..23E

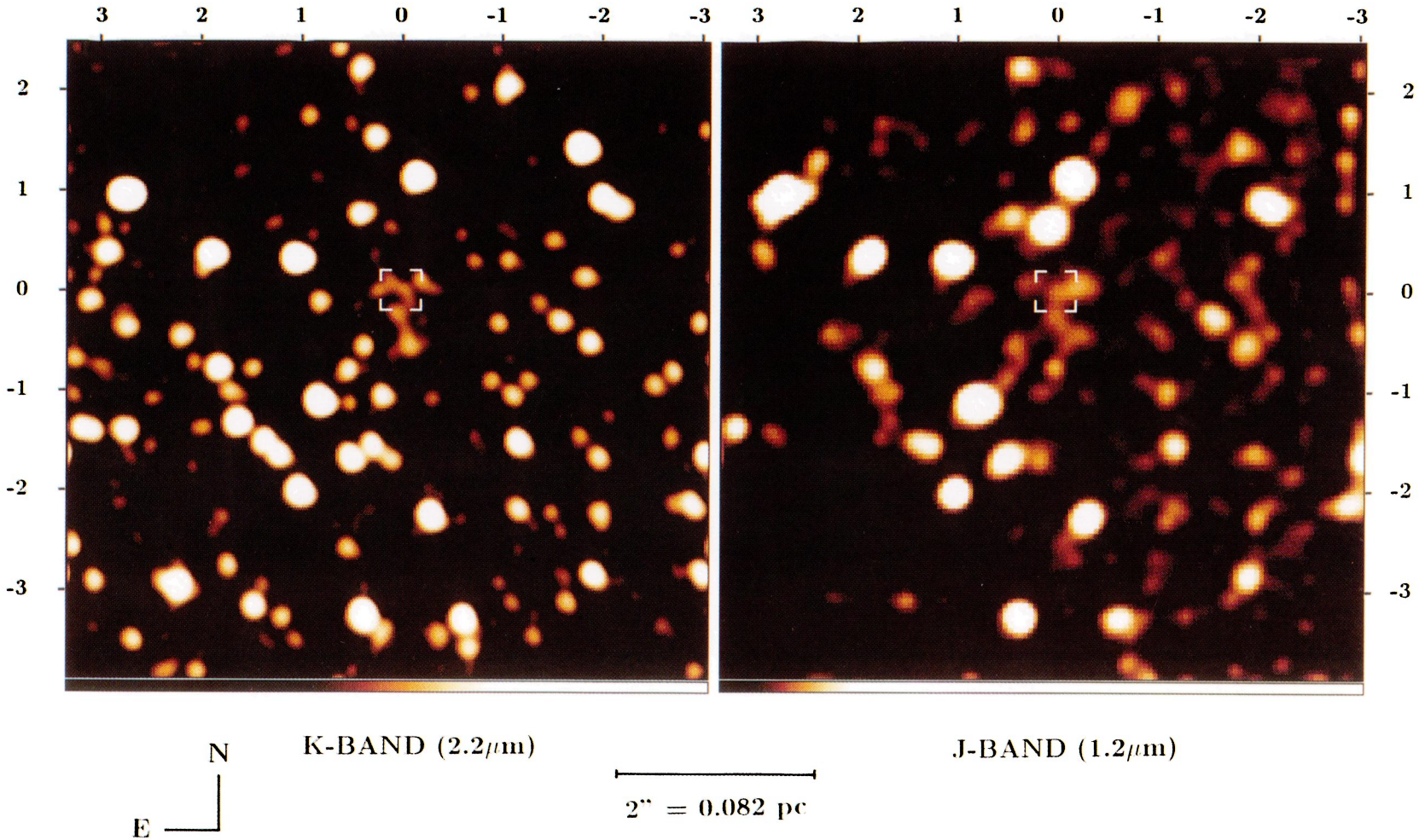

FIG. 2.—*Left*: Color representation of a shift-and-add speckle image reconstruction of the central 3″.2 × 3″.2 centered on Sgr A*(IR) at a wavelength of 2.2 μm (resolution 0″.15 FWHM). *Right*: Same for the *J*-band (1.25 μm) at a resolution of 0″.2 FWHM. The data were taken in 1994 April. The error box for the position of the radio source Sgr A*(R) is indicated. The small cluster of stellar sources within the box is the previously found EW extended near-infrared source Sgr A*(IR).

ECKART et al. (see 445, L23)

© American Astronomical Society • Provided by the NASA Astrophysics Data System

1995ApJ...445L..23E

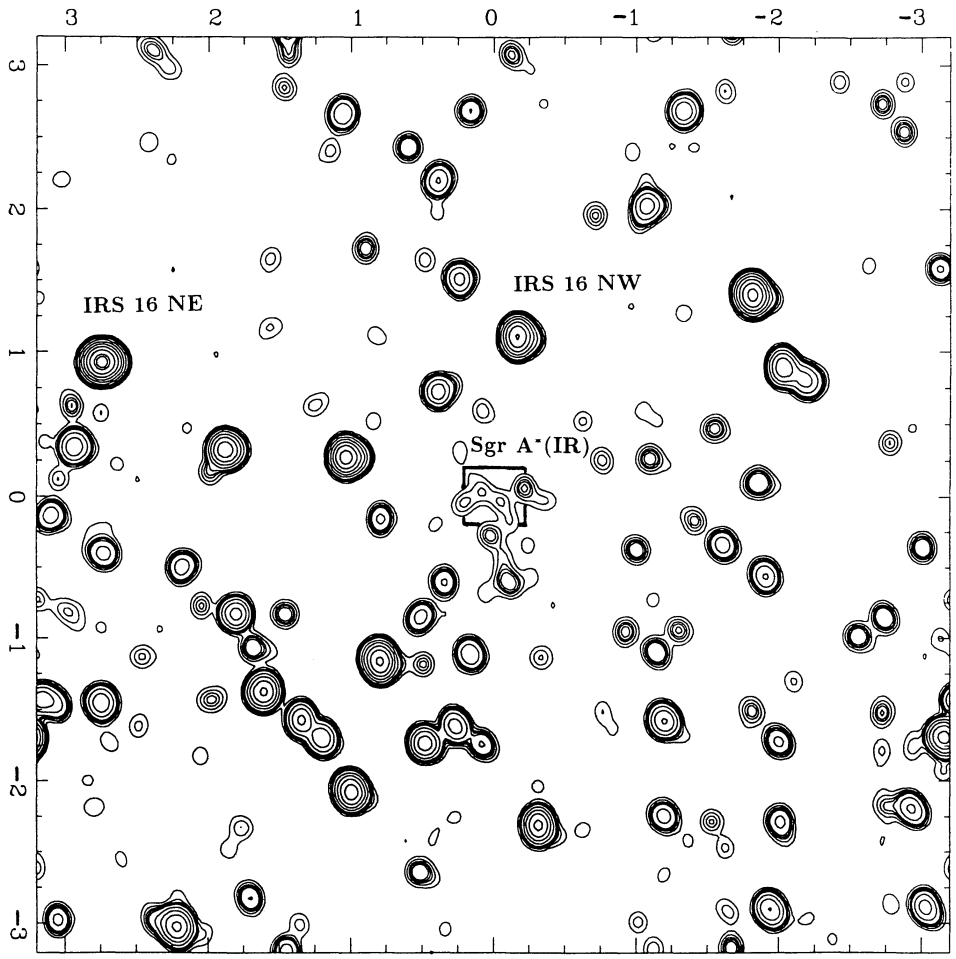

FIG. 1.—Shift-and-add speckle image reconstruction of the central 3″.2 × 3″.2 centered about 1″ south of Sgr A*(IR) at a wavelength of 2.2 μm (resolution 0″.15 FWHM). The data were taken in 1994 April. Several sources are labeled, and the error box for the position of Sgr A*(R) is indicated (see Eckart et al. 1993). The small cluster of stellar sources within the box is the previously found EW extended near-infrared source Sgr A*(IR). The contour levels are 0.15, 0.3, 0.45, 0.65, 0.8, 1, 2, 4, 8, 16, 32, 64, 80, and 100% of the peak brightness of IRS 16NE ($K = 9.0$ or 0.16 Jy).

uum ratios were calculated only within a distance of 0″.4 around the positions of the brighter stars ($K \leq 12$–13) in 0″.4 resolution images. In order to increase the signal-to-noise ratio, we added the CVF and NBF line and line-to-continuum maps. In Figure 3 (Plate L5) we show a combination of the line and line-to-continuum maps for He I and CO, respectively. In the case of our CO band head imaging we could subtract the continuum on only one side of the absorption feature using the CVF data. As a result, our data are also somewhat sensitive to the spectral shape of the continuum. A CO "signal" may thus arise if the spectrum has a downward curvature at $\lambda \approx 2.3$ μm, as it might occur in a featureless blue intrinsic spectrum with a large amount of local extinction. Our identifications of CO absorbers therefore need to be confirmed by spectroscopy which is now underway with our new field imaging spectrograph, 3D (Krabbe et al. 1995).

2.2. *Polarimetric Measurements*

The polarization measurements were carried out with a warm, rotatable wire grid with 4000 lines per millimeter on a 2 mm thick BaF_2 substrate as an analyzer. In sequence we repeatedly recorded a few hundred short-exposure images at five different position angles of the analyzer set 30° apart from each other. After sky subtraction and application of a flat field, the data were calibrated for instrumental effects with the known K-band polarizations of IRS 7 and IRS 1W (3.4% ± 0.5% at P.A. 18° ± 5° and 3.0% ± 1.0% at P.A. 10° ± 7° in a 5″.8 aperture averaging the data given in Lebofsky et al. 1982 and Knacke & Capps 1977). We then calculated the degree and position angle of polarization by fitting a cosine function to the intensities integrated in 0″.25 diameter circular apertures centered on individual sources. Significant polarizations could be established for all 160 sources with $K > 13$. The results are displayed in Figure 4. Typical uncertainties are ±0.5% and 5°.

3. NEW RESULTS

The new data now allow us to study the distribution, $J-K$ colors, and polarization of spectroscopically different sources close to or at the diffraction limit of the NTT. We can also determine properties of the possible counterpart of the compact radio source Sgr A*(R).

3.1. *Properties of Sgr A*(IR)*

Sgr A(IR) is a cluster of compact sources.*—Previous SHARP K-band images had already shown that Sgr A*(IR) is extended ≈0″.5 east-west (Eckart et al. 1993, 1994) or multiple. In good agreement with our previous maps, the new diffraction

© American Astronomical Society • Provided by the NASA Astrophysics Data System

1995ApJ...445L..23E

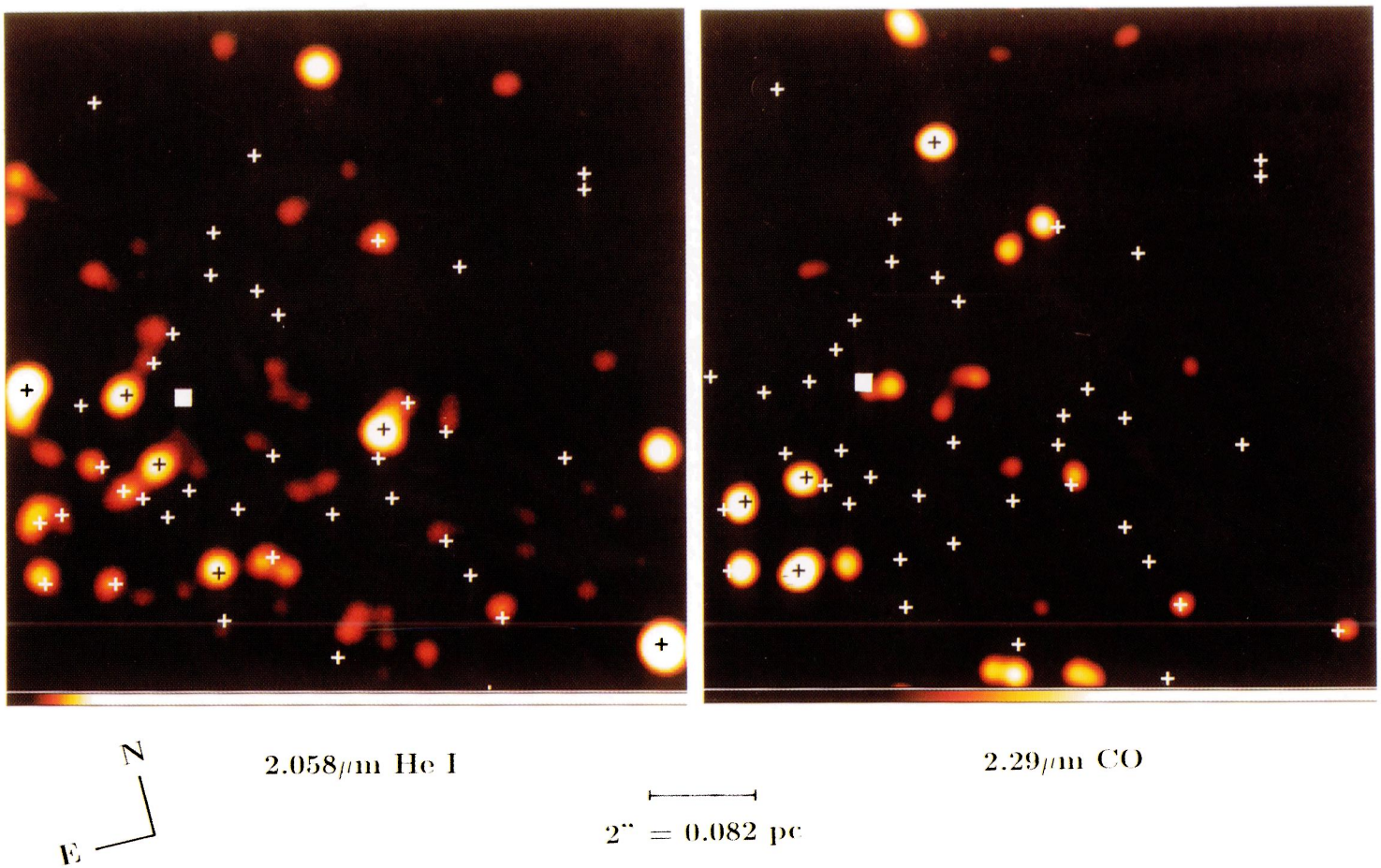

FIG. 3.—False-color representation of the 2.058 μm He I line emission (*left*) and 2.39 μm CO band head absorption (*right*) at a resolution of 0".4. Wavelengths of the on- and off-line channels as well as the algorithm for obtaining the maps are given in the text. Crosses indicate the positions of bright stars. The square indicates the position of Sgr A*(R). The whole field is rotated by 17° such that IRS 7 (cross in the very NE) and the Allen/Forrest star (cross in the very SW) could be observed simultaneously.

ECKART et al. (see 445, L24)

© American Astronomical Society • Provided by the NASA Astrophysics Data System

1995ApJ...445L..23E

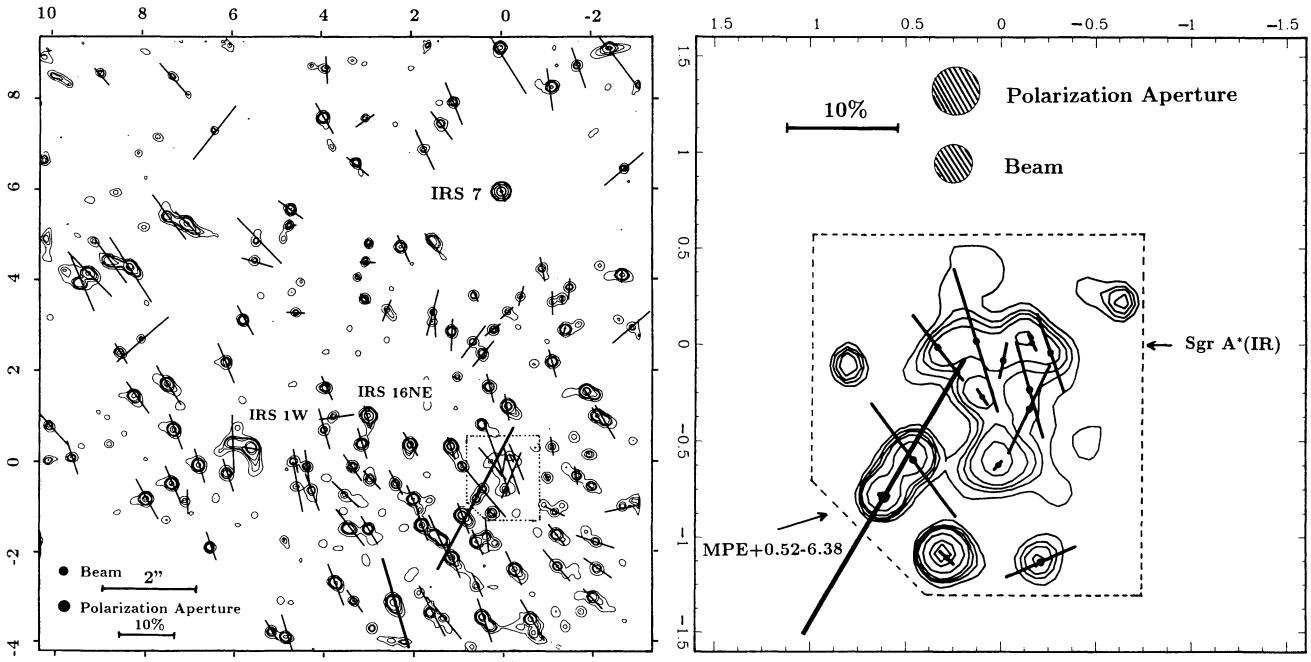

FIG. 4.—*Left*: 0″.2 resolution total intensity images as obtained from the polarization data with the polarization vectors superposed. Two sources show a significantly larger degree of polarization: The source MPE +0.52−6.38 (the number indicate the offset from IRAS 7 in arcseconds) with 29% at −28° and IRS 21 (MPE −8.57+2.20) with 17% at 16°. The mean flux-weighted polarization of all sources in the field of view is 4% at 25°. Typical uncertainties are ±0.5% and 5°. *Right*: 0″.2 resolution zoom of the central 2″ × 2″ containing Sgr A* and the highly polarized source MPE +0.52−6.38.

limited images of the central parsec now clearly reveal that its spatial extent is due to the superposition of at least a half-dozen individual compact components within ≈0″.5 of the nominal position of Sgr A*(R) (box in Figs. 1 and 2) with $K \approx 14$–15. Their projected distances from each other are of the order of our resolution (8×10^{-3} pc or about 1700 A.U. at 8.5 kpc) so that the structure of Sgr A*(IR) is confusion limited at ≈0″.1 resolution.

Sgr A(IR) is not variable.*—In the course of about 3 yr (1991 August to 1994 April) we did not detect any long-term flux variability greater than ±0.25 mag (3 σ) of the total flux of Sgr A*(IR) in the K-band ($m_K \approx 12$ in a 1″ aperture). To test for short-term variability we examined the relative fluxes of IRS 7, IRS 16C, and Sgr A*(IR) in one of our best (1 s exposures; 0″.3 seeing) data sets from 1992 March. On the raw, image motion–compensated frames, we integrated the fluxes over 0″.5 × 0″.5 apertures centered on IRS 7, IRS 16C, and Sgr A*(IR). We then binned the data into intervals of 20 s each. The only residual variations over the course of 60 minutes are <15% for the Sgr A*(IR)/IRS 7 ratio and <7% for the IRS 16C/IRS 7 ratio. The apparent deviations that do appear above the noise in the ratio to IRS 7 of 10% and 5%, respectively, are present in both ratios and are therefore not intrinsic to Sgr A*(IR).

Sgr A(IR) has the same colors as IRS 16 and has no strong spectral features.*—The $J-K$ colors of Sgr A*(IR) as well as the central and northern sources of the IRS 16 cluster are very similar ($J-K = 5.2$) and—most likely due to local extinction variations in the H II region Sgr A West—about 0.5 mag bluer than most other sources that surround the central few arcseconds. This statement holds with the exception of the foreground stars Irr 1 (≈1″ WNW of IRS 16C in Fig. 1) and Irr 2 (e.g., Rosa et al. 1992). There is an obvious lack of J-band sources SE of the line connecting IRS 16NE and IRS 33 probably due to the central arm of the Sgr A West minispiral (e.g., Lo & Claussen 1983). There is no exceptional color gradient across Sgr A*(IR) in our 0″.2 $J-K$ color map and no significant signal at Sgr A*(IR) in the two spectral lines we investigated.

Sgr A(IR) has no large intrinsic polarization.*—At the obtained resolution and sensitivity, the degree and angle of the K-band polarizations of the Sgr A*(IR) sources are similar to those of sources in its vicinity and thus are probably caused by anisotropic absorption by aligned interstellar dust grains along the line of sight to the Galactic center (Lebofsky et al. 1982; Knacke & Capps 1977). An upper limit to the intrinsic polarization of Sgr A*(IR) is about 2%. There is one strongly polarized source at the periphery of the Sgr A*(IR) complex 1″ ± 0″.2 SE of the nominal position of Sgr A*(R): MPE +0.52−6.38 (numbers indicate offset from IRS 7 in arcseconds) with 29% at −28°. Its color is similar to sources in its vicinity. Its large polarization is therefore unlikely due to local anisotropic absorption but more likely caused by scattering.

Sgr A(IR) is likely a central stellar condensation and Sgr A*(R) is dark.*—Given our new findings only the combination of its position and the large surface density of objects make Sgr A*(IR) now look peculiar with respect to the surrounding stars. We conclude that Sgr A*(IR) is most likely a local clustering of moderately luminous stars with $M_K \approx -3$. These could either be early-type main-sequence (B0 V: $\approx 10^{4.4}\ L_\odot$) or late-type (K2–4 III: $\approx 10^{2.3}\ L_\odot$) giant stars. To answer which—if any— of the half-dozen sources in Sgr A*(IR) can be identified with Sgr A*(R) the present ±0″.2 uncertainty of the relative positioning of the radio and infrared frames has to be substantially improved (e.g., Eckart et al. 1993; Yusef-Zadeh & Melia 1992). If the 1–3 × $10^6\ M_\odot$ central mass concentration within 5″ (0.2 pc) of Sgr A* (Genzel et al. 1994) refers to Sgr A*(R), its mass-to-luminosity ratio presently is at least $\approx 100\ M_\odot/L_\odot$.

Number density distribution.—Following Eckart et al. (1993)

© American Astronomical Society • Provided by the NASA Astrophysics Data System

1995ApJ...445L..23E

we computed the radial distribution of number surface density averaged in 0".3 wide annuli centered on Sgr A*(R) for 600 sources with $6.8 < m_K < 15$ and 264 sources with $6.8 < m_K < 13.8$. As in Eckart et al. (1993, 1994) the number distribution is centered within $\pm 1''$ ($3\ \sigma$) on Sgr A*(R), and sources with $K < 13.8$ at a distance $\leq 10''$ from the centroid follow an isothermal distribution with a core radius of ≈ 0.2 pc (5"). Including the faintest sources ($K < 15$) indicates a somewhat flatter distribution (core radius ≈ 0.3 pc) between 2" and 10". However, a proper correction for crowding in the central few arcseconds has not been done which would increase the central surface density. At the same time Sgr A*(IR) now shows up as a central excess (10 sources per arcsec^2) above the best fitting isothermal distribution (three to four sources per arcsec^2). This excess is presently only significant at the 2 σ level, above that of the flat (isothermal) distribution, however. Sgr A*(IR) may thus be a central cusp in the overall stellar distribution, but substantial improvements in both angular resolution (confusion) and sensitivity are required in order to verify this possibility with better statistical significance.

3.2. *The Stellar Content of the Central Parsec*

The mean flux-weighted polarization of all sources in the central 0.25 pc with $K < 13$ is 4% at 25° in agreement with data in Lebofsky et al. (1982). This is within 7° parallel to the Galactic plane. Most of the polarizations therefore are caused via absorption by aligned interstellar dust grains in the plane. Two sources show a significantly larger degree of polarization: The source MPE $+0.52-6.38$ (see above) and IRS 21 (MPE $-8.57+2.20$) with 17% at 16°.

IRS 21 has a very red 2 μm spectrum without strong spectral lines (Krabbe et al. 1995), suggesting it is heavily absorbed or has a disk. Polarizations as large as observed can be obtained via scattering of the radiation of a central source by dense asymmetrically distributed dust (Elsässer & Staude 1978). IRS 21 may therefore be a young massive star that has recently formed in the central part of the Sgr A West gas filaments.

From our line maps (Fig. 3) it is possible, for the first time, to identify individual early-type stars (He I line emission) and late-type stars (CO absorption) in the central few arcseconds. The He I line-to-continuum map in Figure 3 clearly reveals about 15 He I emission-line stars (see also Krabbe et al. 1991, 1994; Genzel et al. 1994). In particular our data clearly show that IRS 16NE, IRS 16C, IRS 16SW, and IRS 16NW are truly He I stars and not part of an extended distribution. The IRS 16 complex thus is in fact, as proposed by Krabbe et al. (1991, 1994), the central concentration in the hot star cluster. The CO 2.3 μm map shows for the first time about 15 candidates as potential CO absorption stars with $K \leq 12.5$ in the inner 10". Such stars could either be solar mass, late-M giants or intermediate-mass (2–8 $M_\odot$) AGB stars. About 20 objects with $K \leq 12.5$ which do not show significant features in the He I or CO line may either be main-sequence O stars, B/A/F supergiants, or embedded young stars.

Since we have detected a substantial number of fairly bright CO absorption sources within the central 10", the drop in CO band head strength (Sellgren et al. 1990) is likely caused not by the disappearance of CO sources but by the additional presence of bright early-type stars, including the He I emission-line stars. This conclusion gains additional support from the fact that the band head strength as a function of radius as mapped by Sellgren et al. (1990) is similar to the variation of the ratio of the faint star ($11 \leq K \leq 14$) to total ($K \leq 14.5$) SHARP surface brightness or the variation of surface brightness of stars with CO absorption to total surface brightness as derived by Allen (1994).

We thank N. Ageorges and M. Löwe for help in taking the SHARP data. N. A. helped designing and installing the polarizer on the SHARP camera. We also thank F. Lo, P. G. Mezger, M. J. Rieke, and G. H. Rieke for comments and fruitful discussions. We are grateful to ESO for technical support of the SHARP system at the NTT.

REFERENCES

Allen, D. A. 1987, in The Galactic Center, ed. D. Backer (New York: AIP), 1
———. 1994, in The Nuclei of Normal Galaxies, ed. R. Genzel & A. I. Harris (Dordrecht: Kluwer), 293
Allen, D. A., Hyland, A. R., & Hillier, D. J. 1990, MNRAS, 244, 706
Bailey, M. E. 1980, MNRAS, 190, 217
Christou, J. C. 1991, Exp. Astron., 2, 27
Close, L. M., McCarthy, D. W., & Melia, F. 1995, ApJ, 439, 682
Eckart, A., Genzel, R., Hofmann, R., Sams, B. J., & Tacconi-Garman, L. E. 1993, ApJ, 407, L77
Eckart, A., Genzel, R., Hofmann, R., Sams, B. J., Tacconi-Garman, L. E., & Cruzalebes, P. 1994, in The Nuclei of Normal Galaxies, ed. R. Genzel & A. I. Harris (Dordrecht: Kluwer) 305
Eckart, A., Genzel, R., Krabbe, A., Hofmann, R., van der Werf, P. P., & Drapatz, S. 1992, Nature, 335, 526
Elsässer, H., & Staude, H. J. 1978 A&A, 70 L3
Genzel, R., Hollenbach, D. J., & Townes, C. H. 1994, Rep. Progr. Phys., 57, 417
Herbst, T. M., Beckwith, S. V. W., & Shure, M. 1993, ApJ, 411, L21
Hofmann, R., Blietz, M., Duhoux, P., Eckart, A., Krabbe, A., & Rotaciuc, V. 1993, in Progress in Telescope and Instrumentation Technologies, ed. M. H. Ulrich (ESO Rept. 42), 617
Knacke, R. F., & Capps, R. W. 1977, ApJ, 216, 271
Krabbe, A., et al. in Infrared Astronomy with Arrays (3), ed. I. McLean (Dordrecht: Kluwer), 484
Krabbe, A., Genzel, R., Drapatz, S., & Rotaciuc, V. 1991, ApJ, 382, L19
Krabbe, A., et al. 1995, in preparation
Lebofsky, M. J., Rieke, G. H., Deshpande, M. R., & Kemp, J. C. 1982, ApJ, 263, 672
Lo, K. Y. 1989, in The Center of the Galaxy, ed. M. Morris (Dordrecht: Kluwer), 537
Lo, K. Y., & Claussen, M. J. 1983, Nature, 306, 647
Rosa, M. R., Zinnecker, H., Moneti, A., & Melnick, J. 1992, A&A, 257, 515
Sellgren, K., McGinn, M. T., Becklin, E. E., & Hall, D. N. B. 1990, ApJ, 359, 112
Yusef-Zadeh, F., & Melia, F. 1992, ApJ, 385, L41

Note added in proof.—A comparison of recent 5 GHz VLA A-array images (taken by Zhou, Shudong, & K. Y. Lo) shows that within an error of 0".1 the radio position of Sgr* agrees with the position of the faint source southwest of the central tip of the M-shaped distribution of stellar sources in the error box of Fig. 1 (5".60 south and 0".13 west of IRS 7). The radio and infrared rest frames were combined using IRS 7, IRS 13, and IRS 1W.

© American Astronomical Society • Provided by the NASA Astrophysics Data System